INTERNATIONAL JOURNAL OF HYDROGEN ENERGY XXX (2016) 1–10

Available online at www.sciencedirect.com

ScienceDirect

journal homepage: www.elsevier.com/locate/he

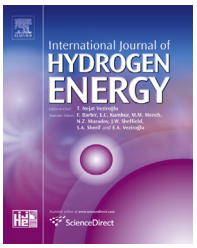

Red mud enhanced hydrogen production from pyrolysis of deep-dewatered sludge cakes conditioned with Fenton's reagent and red mud

Jian Song [a,1], *Jiakuan Yang* [a,b,*], *Sha Liang* [a,1], *Yafei Shi* [a], *Wenbo Yu* [a], *Chao Li* [a], *Xinyu Xu* [a], *Jun Xiao* [a], *Ruonan Guan* [a], *Nan Ye* [a], *Xu Wu* [a], *Huijie Hou* [a], *Jingping Hu* [a], *Jiukun Hu* [c], *Bo Xiao* [a]

[a] *School of Environmental Science & Engineering, Huazhong University of Science and Technology, Wuhan, Hubei, 430074, PR China*

[b] *State Key Laboratory of Coal Combustion, Huazhong University of Science and Technology, Wuhan, Hubei, 430074, PR China*

[c] *Dongjiang Environment, Co., Ltd., Shenzhen, Guangdong, 518057, PR China*

ARTICLE INFO

Article history:
Received 26 February 2016
Received in revised form
6 June 2016
Accepted 27 June 2016
Available online xxx

Keywords:
Sewage sludge
Catalytic pyrolysis
Red mud
Gasification
Hydrogen production

ABSTRACT

This study investigated the pyrolytic performances of deep-dewatered sludge cakes which were previously conditioned with Fenton's reagent and red mud. The pyrolytic products, including fuel gas, tar and solid char, were characterized by GC, GC-MS and FTIR. The results showed that pyrolysis of sludge cakes conditioned with Fenton's reagent and red mud produced more gas, especially higher H_2 yield, compared with pyrolysis of raw sludge. In addition, red mud promoted PAHs formation and tar re-formation through side-chain-cleaving, dehydrogenation, polycondensation and aromatization of hydrocarbon during the pyrolysis, resulting in enhancement of the H_2 yield. The sharp decrease in the absorbance of $C-H_{aromatic}$ group of chars from the conditioned cakes implied that red mud could intensify the cracking and re-formation of aromatics. The higher the iron oxide content in red mud was, the better catalytic efficiency in the decomposition of organics and tar re-formation was, which led to more H_2 production.

Introduction

The generation of sewage sludge, a by-product of municipal wastewater treatment, has been rapidly increasing in China, due to fast urbanization. Over 80% of sewage sludge in China is not properly disposed of and has become a source of secondary pollution to the environment [1]. Presence of the extracellular polymeric substances (EPS), which has a high affinity for water, makes dewatering and subsequent treatment and disposal of sewage sludge extremely difficult [2]. Effective reduction of its water content before final treatment and/or disposal is of pivotal importance for the

* *Corresponding author*. School of Environmental Science and Engineering, Huazhong University of Science and Technology, Wuhan, 430074, PR China.
E-mail address: jkyang@mail.hust.edu.cn (J. Yang).
[1] These authors contributed equally to this work.

http://dx.doi.org/10.1016/j.ijhydene.2016.06.217
0360-3199/

Abbreviation list

DS	Dry Solid
EPS	Extracellular Polymeric Substances
Fenton	Dewatered cake conditioned by Fenton's reagent alone
Fenton-RD	Dewatered cake conditioned by Fenton's reagent with red mud
Fenton-RD1	Dewatered cake conditioned by Fenton's reagent with red mud produced from the bauxite of Australia
Fenton-RD2	Dewatered cake conditioned by Fenton's reagent with red mud produced from the bauxite of Indonesia
Fenton-RD3	Dewatered cake conditioned by Fenton's reagent with red mud produced from the bauxite of China
FTIR	Fourier Transform Infrared Spectroscopy
GC	Gas Chromatography
GC-MS	Gas Chromatography-Mass Spectrometer
MS	Mass Spectrometer
NIST	National Institute of Standards and Technology
PAHs	Polyaromatic Hydrocarbons
RD1	Red mud produced from the bauxite of Australia
RD2	Red mud produced from the bauxite of Indonesia
RD3	Red mud produced from the bauxite of China
RS	Raw Sludge
TCD	Thermal Conductivity Detector
TG-FTIR	Thermogravimetry Fourier Transform Infrared
TIC	Total Ion Chromatogram
XRD	X-Ray Diffraction

sewage sludge management. The traditional dewatering technology commonly using polymer as a conditioner followed by centrifugal filter or belt filter can only reduce the water content of sludge to approximately 80 wt% [3], which fails to meet the maximum water content limit for landfilling in China [4]. Moreover, higher water content of dewatered cake causes higher energy consumption and higher run cost in the thermal conversion technologies for the sequent treatment of sludge [5]. Our previous work has demonstrated that sewage sludge conditioned with Fenton's reagent and red mud could produce deep-dewatered sludge cakes with water content of less than 60 wt% [6].

Landfilled or land utilization is an alternative for the sequence treatment and disposal of the deep-dewatered sludge cakes. However, apart from the occupation of valuable landfill capacity, the presence of heavy metals, organic contaminants and pathogens in sewage sludge will pose potential adverse impacts on agricultural applications and jeopardize soil and groundwater. Pyrolysis of sewage sludge, which could transfer organic matters to clean fuel gases such as H_2, CH_4 and other useful products, provides an alternative to sewage sludge management [7]. Characteristics and kinetics of sewage sludge pyrolysis has been investigated by thermogravimetry Fourier Transform Infrared (TG-FTIR) analysis, it was found that pyrolysis occurred mainly at about 150–550 °C and the pyrolysis gases comprised mainly CO, CO_2, CH_4 and light hydrocarbons [8]. Some researchers also studied the mechanism of pyrolysis of the wet sewage sludge in a tubular furnace and used Diels–Alder reaction model to interpret its pyrolytic performances [9]. But the low yield of gas especially H_2 yield from the pyrolysis of sewage sludge is still a common problem that needs to be solved urgently. Thus, some researchers investigated the improvement of hydrogen production using catalyst, such as calcium oxide based catalyst or steam during sewage sludge pyrolysis as seen in Table 1 [5,9–12].

Red mud is an alkaline industrial waste produced in the process of alumina extraction from bauxite leaching with sodium solution, and approximately 120 million tons of red mud are produced annually worldwide [13]. As the largest producer of red mud in the world, China confronts severe challenges in red mud disposal [14]. Typical chemical compositions of red mud are Fe_2O_3, Al_2O_3, SiO_2, TiO_2, Na_2O and CaO, depending on both the bauxite source and the alumina production process; and the mineralogical compositions of red mud from the Bayer process are mainly hematite (Fe_2O_3), gibbsite ($Al(OH)_3$), quartz(SiO_2) and other Si–Al chemical compounds [15]. Due to the abundance of metallic oxide in red mud, red mud has been used as a catalyst in various reactions, such as hydrodechlorination of chlorine-containing organics [16], hydrogenation of coals and some waste residues [17], and pyrolysis of biomass and plastic for the production of oil [18]. Furthermore, it has been reported that red mud could promote the decomposition of biomass or hydrocarbon to produce more fuel gas, especially H_2 [18–21]. However, researches on using red mud as a catalyst for pyrolysis of sludge cakes were not reported in literatures.

The aim of the present study was to investigate the pyrolytic performance and potential catalytic effect of red mud on deep-dewatered sludge cakes which were previously conditioned with Fenton's reagent and red mud. The objectives of this study were: (1) to demonstrate the role of red mud in the enhanced efficiency of gas yield, especially H_2 yield, during the pyrolysis, and (2) to compare the catalytic ability of red mud with different chemical and mineralogical compositions.

Materials and methods

Materials and sample preparation

A mixture of primary sludge and secondary sludge from Tangxunhu wastewater treatment plant in Wuhan, China was used as the raw sludge in this study. The water content of the raw sludge (abbreviated as RS) after sludge thickening was above 97 wt%. Results of the proximate and ultimate analysis of RS are summarized in Table 2. The proximate analyses of RS and other samples were examined according to Chinese national standards of proximate analysis of coal(GB/T 212-2008), and the ash content was measured under the condition that the sample was burned in a muffle furnace with the temperature increased from room temperature to 500 °C in more than 30 min and then continued to heat up to 815 °C and kept at 815 °C for 1 h, and the ultimate analyses of all the samples

Please cite this article in press as: Song J, et al., Red mud enhanced hydrogen production from pyrolysis of deep-dewatered sludge cakes conditioned with Fenton's reagent and red mud, International Journal of Hydrogen Energy (2016), http://dx.doi.org/10.1016/j.ijhydene.2016.06.217

Table 1 – Related research on hydrogen-rich gas produced from pyrolysis of sewage sludge.

Materials	Accelerant	Conditions	Results	Reference
Hydrochar derived from sewage sludge	Steam	700 to 1000 °C	The maximum volume of H_2 accounts for 35%	[5]
Dewatered sewage sludge	Steam	600 to 1000 °C	The maximum volume of H_2 accounts for 31.6%	[9]
Dewatered sewage sludge	CaO	380 °C	H_2 yield could grow nearly 6-fold	[10]
Dried sewage sludge	Ni-impregnated activated carbon	750 °C	The maximum volume of H_2 accounts for 31.3%	[11]
Dewatered sewage sludge	Steam	600 to 800 °C	The volume ratio of H_2 of dewatered sewage is much higher than dried sludge	[12]

Table 2 – Proximate and ultimate analysis of different sewage sludge samples.

Materials	Proximate analysis (wt%)				Ultimate analysis (wt%)[b]				
	Moisture	Volatiles[a]	Ash[a]	Fixed carbon[a]	C	H	N	S	O[c]
RS	97.18	52.91	42.86	4.22	27.01	4.44	4.79	1.40	19.50
Fenton	64.03	59.04	38.36	2.60	27.99	4.60	5.23	1.70	22.12
Fenton-RD1	57.81	46.58	52.47	1.01	21.75	3.83	4.09	1.07	16.79
Fenton-RD2	58.84	48.11	50.96	0.93	21.71	3.90	4.09	1.14	18.20
Fenton-RD3	57.44	49.51	48.87	1.62	22.69	4.04	4.27	1.23	18.90

[a] Dry basis.
[b] Dry and ash free basis.
[c] Calculated by difference.

were measured using an elemental analyzer(Vario Micro cube, Elementar, Germany).

H_2SO_4 (Analytical grade, Xinyang Chemical Company, China) was used to adjust the initial pH of RS to 5.0 before conditioning. To form the Fenton's reagent, industrial-grade Fe^{2+} (prepared from a solution of $FeSO_4$) and H_2O_2 were obtained from Sinopharm Chemical Reagent Company, China. Three types of red mud was taken from three alumina plants using the Bayer process in China, and their chemical compositions were measured by X-ray Fluorescence Spectrometer (Axios^{mAx}, PANalytical, Netherlands) are tabulated in Table 3. The chemical compositions of red mud used depend on the source of bauxite ores (i.e., Australia, Indonesia and China) as shown in Table 3. Three types of red mud produced from the bauxite of Australia, Indonesia and China are noted as RD1, RD2, and RD3, respectively. These red mud samples were used as the skeleton builder during sludge conditioning after red mud samples were milled and sieved to particles less than 1 mm. The mineral phases of these types of red mud were analyzed by powder X-ray diffractometry (XRD), using an X'Pert ProXRD (Philips, PANalytical B.V., Netherlands) operated at 300 mA, 40 kV with a scanning rate of 0.2785°/s for 2θ in the range from 5° to 75°. The XRD patterns of these three kinds of red mud samples are shown in Fig. 1. As identified in the XRD patterns, the main mineral phases of red mud are hematite (Fe_2O_3), gibbsite ($Al(OH)_3$) and quartz, which is consistent with the previous literatures [15].

The dewatering process was followed procedures in our previous study [6]. Raw sludge was conditioned with Fenton's reagent (32 mg Fe^{2+}/g dry solid (DS) combined with 34 mg H_2O_2/g DS) and red mud (275 mg/g DS), and followed by mechanically dewatering using a diagram press filter under a pressure of 0.8 MPa. The details of the dewatering procedures can be found in our previous study [6]. The deep-dewatered cakes, previously conditioned with Fenton's reagent and RD1, RD2 and RD3 were referred to Fenton-RD1, Fenton-RD2 and Fenton-RD3, respectively. The dewatered cake conditioned with Fenton's reagent alone was referred to Fenton as the control. The results of proximate and ultimate analysis on Fenton, Fenton-RD1, Fenton-RD2 and Fenton-RD3 are also shown in Table 2. As shown in Table 2, the contents of volatiles and fixed carbon of cakes conditioned with Fenton's reagent and red mud are smaller, when compared to the RS and the Fenton, due to the addition of inorganic red mud. All cake samples and the RS were dried at 105 °C to a constant weight, and then milled and sieved to 75 μm in particle size. 10.0 g of sample, on a dry basis of raw sludge, was subjected to the treatment in each of the subsequent experiment to ensure

Table 3 – Chemical compositions of red mud from three different bauxite ore sources (wt%).

Red mud	Fe_2O_3	Al_2O_3	TiO_2	MgO	Na_2O	K_2O	SiO_2	CaO	LOI[a]
RD1 (Australian)	40.85	13.20	7.12	0.12	8.23	0.04	11.07	6.03	10.08
RD2 (Indonesian)	33.88	17.89	0.72	0.10	12.18	0.37	19.43	2.66	12.84
RD3 (Chinese)	9.48	24.50	2.92	1.00	11.46	0.88	20.38	12.86	15.40

[a] Loss of ignition at 1200 °C.

Please cite this article in press as: Song J, et al., Red mud enhanced hydrogen production from pyrolysis of deep-dewatered sludge cakes conditioned with Fenton's reagent and red mud, International Journal of Hydrogen Energy (2016), http://dx.doi.org/10.1016/j.ijhydene.2016.06.217

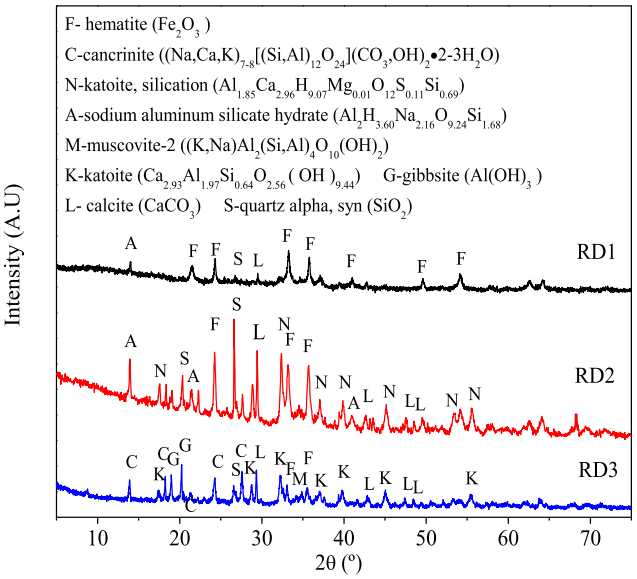

Fig. 1 – The XRD patterns of red mud samples from three different sources.

consistency and comparability. Three parallel samples for each group were studied.

Experimental apparatus and procedure

Experiments were carried out in a horizontal quartz reactor (1200 mm length × 70 mm I.D.), heated by an electrical tube furnace as shown in Fig. 2. The whole pyrolysis system consists of a quartz tube, a cooling system for condensation of water and condensable organic vapors, a gas cleaning/drying system, a wet gas meter and a gas sampling bag.

Pyrolysis of the deep-dewatered sludge cake was performed as follows: temperature of the furnace was firstly elevated to a pre-set temperature (three temperature levels: 700, 800 and 900 °C); sludge sample was then introduced to one side of the reactor with a nitrogen flow (99.99%, 100 mL/min) throughout the pyrolysis process. The sample was injected into the reaction zone, when an inert atmosphere was formed and an isothermal environment kept for 20 min. Volatiles evaporated from the sample first passed through two consecutive condensers in an ice water bath to collect the condensable fraction, and then passed a filter packed with absorbent cottons and allochroic silica gel to remove dust and water. Finally, the non-condensable gas was collected in a sample bag.

The gas collected in the sample bag was analyzed by a gas chromatograph (Agilent 7820A, Agilent, USA) equipped with a TCD detector. Tar in the condensers and the connecting tube was collected as described below: the condensers and the connecting tube were washed by dichloromethane and filtered to remove the particles; The extracted liquid was poured into a separating funnel to separate water and the organic phase that consisted of tar and dichloromethane; Finally, the organic phase was heated in a water bath at 60 °C to remove dichloromethane, and the tar was left and characterized by GC-MS (Agilent 7890A/5975C, Agilent, USA). The gas chromatography (GC) was fitted with a 30 m × 0.25 mm capillary column, and coated with a 0.25-μm thick film containing of 5% phenyl methyl silox (HP-5 MS). Helium was the carrier gas with a flow rate of 1 mL/min and the split flow was 50 mL/min with a split ratio of 50:1. The initial temperature of the oven was 50 °C and kept isothermal for 2 min, and then it was heated to 300 °C with an increase rate of 10 °C/min and kept isothermal for 10 min. The injector temperature was 250 °C, and the temperature of Mass Spectrometer (MS) source and quad were set at 230 °C and 150 °C, respectively. The test was conducted at a full-scan mode with mass to charge (m/z) ratios from 30 to 550, and the delay time of the solvent was 4 min. The NIST (National Institute of Standards and Technology) mass spectral data library was used to identify chromatographic peaks, and the relative percentage content was calculated by the peak area of Total Ion Chromatogram (TIC).

When the furnace was cooled down to room temperature, the solid char was taken out from the reactor and then ground to fine particles. The char powder was mixed with KBr powder at a mass ratio of 1:100, and the mixture was pressed to a pellet for Fourier Transform Infrared Spectroscopy (FTIR) (VERTEX70, Bruker, German) with a spectral resolution at 4 cm^{-1}. For comparison, raw sludge sample was also analyzed by FTIR under the same conditions. Pyrolytic performances of five samples were studied by thermosgravimetric analysis

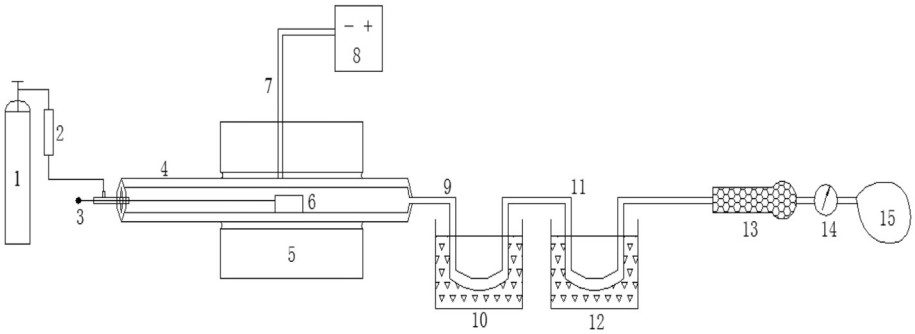

1-high grade pure nitrogen source; 2-gas flowmeter; 3-metal bar; 4-quartz reactor; 5-tubular furnace; 6-corundum boat; 7-thermocouple; 8-thermostat; 9,11-U-shape tube; 10,12-ice bath; 13-filter and dryer; 14-wet gas meter; 15-gas bag

Fig. 2 – Schematic diagram of the tubular furnace pyrolysis system.

Please cite this article in press as: Song J, et al., Red mud enhanced hydrogen production from pyrolysis of deep-dewatered sludge cakes conditioned with Fenton's reagent and red mud, International Journal of Hydrogen Energy (2016), http://dx.doi.org/10.1016/j.ijhydene.2016.06.217

using a thermogravimetric analyzer (SDT-Q600, TA Instrument, USA). During each experiment, the sample was heated to 1000 °C from room temperature with an increase of 20 °C/min under the protection of nitrogen with a flow rate of 100 mL/min.

Experimental data processing method

In order to compare the gas production ability of different sludge cakes, the gas yield per organic matter (m^3/g dry organic matter) was applied as an evaluation criterion to ensure the reliability and veracity of the results. Tar from sludge cake pyrolysis is a complex mixture which contains numerous organic compounds. Lacking of appropriate standard mixture leads to difficulties in setting calibration for a MS detector [22]. In this study, all tests were carried out under the same conditions, and a semi-quantitative method, by means of integrating area of the chromatographic peaks, was used to determine the amount of a specific compound and compare its changing trend with respect to conditions [23].

Results and discussion

Thermal analysis

The Thermal Gravity Analysis (TGA) and Differential Thermal Gravity (DTG) curves of deep-dewatered cakes and the RS sample are shown in Fig. 3. As shown in Fig. 3 (a), the final lost weight was as follows: 55.60% (RS), 53.46% (Fenton), 51.31% (Fenton-RD1), 52.17% (Fenton-RD2) and 51.12% (Fenton-RD3). Cakes conditioned with Fenton's reagent and red mud lost less weight than the RS and that conditioned with Fenton's reagent alone because of the addition of red mud. The weight loss of the RS has only one stage with a weight loss of 49.15 wt% (Fig. 3(b)). In addition, the weight losses of all the cakes with conditioners can be divided into three stages, and the details of weight losses of the RS and other four cakes can be seen in Table S1. From all the above information, it can be found that the organic decomposition of all the cakes was mainly occurred at the temperature of 200 °C–600 °C. During the main weight loss stage, the conditioner of three Fenton-RD would also influence the activation energy of thermal decomposition reactions, as it can be seen from the weight loss peaks in Fig. 3(b). But the addition of conditioners would change the decomposed performances. The conditioned cakes have an extra stage below 100 °C, which can be attributed to the evaporation of water existed in the sludge surface. Because Fenton's reagent has a strong oxidizing ability which could change the organic compositions and structures of conditioned cakes, making it more 'fluffy' and easier to absorb water in the air before put into the TGA instrument than the RS, and Fenton's reagent could also change the combinatorial forms of water [6], which makes water more easier to release, compared to the RS during the heating process. Furthermore, the conditioned cakes have an additional weight loss stage among 700–900 °C, compared with the RS, which was the result of decomposition of nonbiodegradable organics and inorganics in Fenton's reagent and red mud. So, the temperatures of 700, 800 and 900 °C were chosen as the test temperatures in this paper.

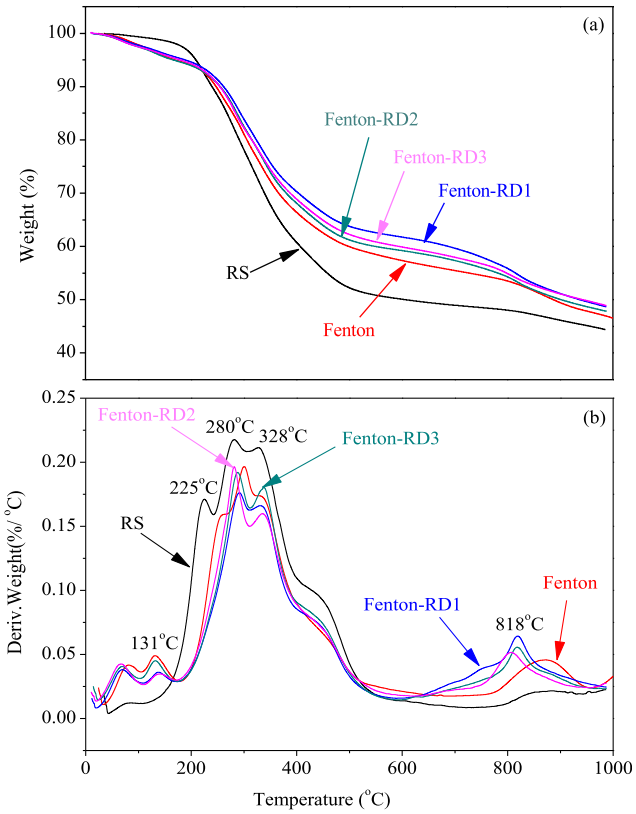

Fig. 3 – TG and DTG curves of five samples: (a) TG curves, and (b) DTG curves.

Gas production

Fig. 4 shows the gas yield (m^3/g of dry organic matter) of the RS and four dewatered sludge cakes at 700, 800 and 900 °C. As shown, the gas yields of five samples increased as the temperature increased, and the gas yields of three samples conditioned with Fenton-RD were higher than the RS and the

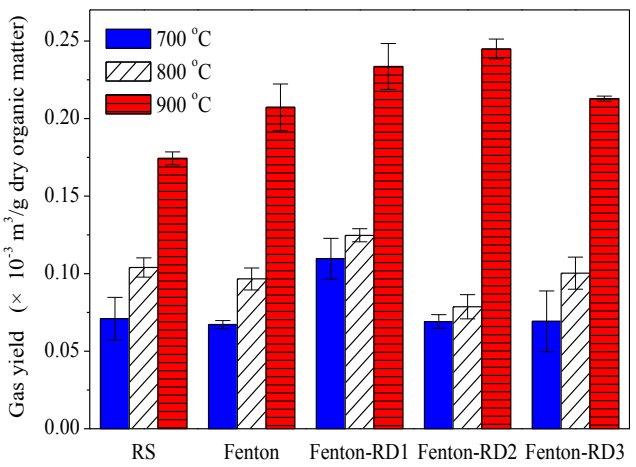

Fig. 4 – Gas yields of the RS and the other four sludge cakes conditioned with Fenton alone, Fenton-RD1, Fenton-RD2, and Fenton-RD3.

Please cite this article in press as: Song J, et al., Red mud enhanced hydrogen production from pyrolysis of deep-dewatered sludge cakes conditioned with Fenton's reagent and red mud, International Journal of Hydrogen Energy (2016), http://dx.doi.org/10.1016/j.ijhydene.2016.06.217

Fenton alone, especially at 900 °C. This probably was due to the influence of inorganic metal oxides such as TiO_2 and Fe_2O_3 in red mud, which can enhance the pyrolytic process [24,25]. Compared to RS and Fenton samples, the gas yield of Fenton-RD1 was 54.5% and 63.3% higher at 700 °C, respectively; and 19.9% and 29.1% higher at 800 °C, respectively. While the gas yields of Fenton-RD2 and Fenton-RD3 were slightly lower, compared to RS and Fenton samples at 700 °C and 800 °C. However, under 900 °C, all the gas yields of Fenton-RD1, Fenton-RD2 and Fenton-RD3 samples were higher than those of both the RS and the Fenton samples. Fenton-RD1 sample exerted a better performance in promoting gasification during the sludge pyrolysis under all three temperatures tested, while Fenton-RD2 and Fenton-RD3 only performed well at 900 °C. It might be attributed to the difference in the highest content Fe_2O_3 and TiO_2 content in RD1, as presented in Table 3.

The gas compositions from pyrolysis are shown in Fig. 5. As shown, the pyrolysis gas from all the sewage sludge samples mainly consisted of H_2, CH_4, CO, CO_2, and some C_{2-3} hydrocarbons. Overall, the H_2, CH_4, and CO yields of Fenton-RD conditioned sludge samples were almost higher than those of the RS and the Fenton's reagent conditioned sample, while the C_{2-3} hydrocarbons yield was lower. H_2 is often considered as the cleanest fuel gas because its combustion product is only

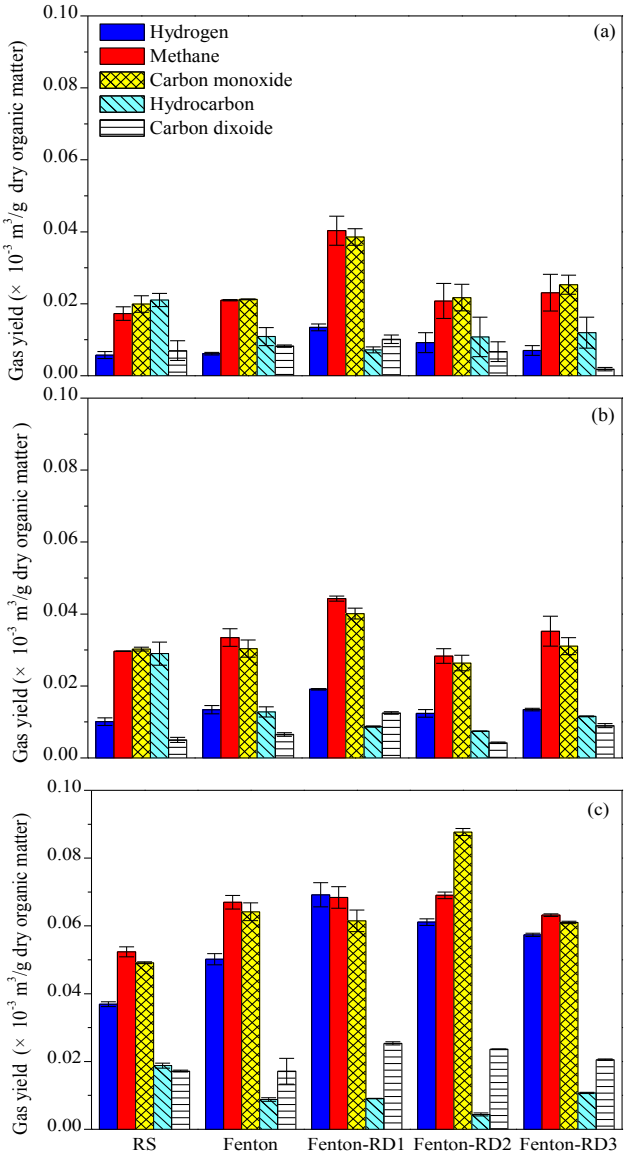

Fig. 5 – Gas compositions from the pyrolysis of the RS and the other four sludge cakes conditioned with Fenton alone, Fenton-RD1, Fenton-RD2, and Fenton-RD3 at three temperatures: (a) 700 °C, (b) 800 °C, and (c) 900 °C.

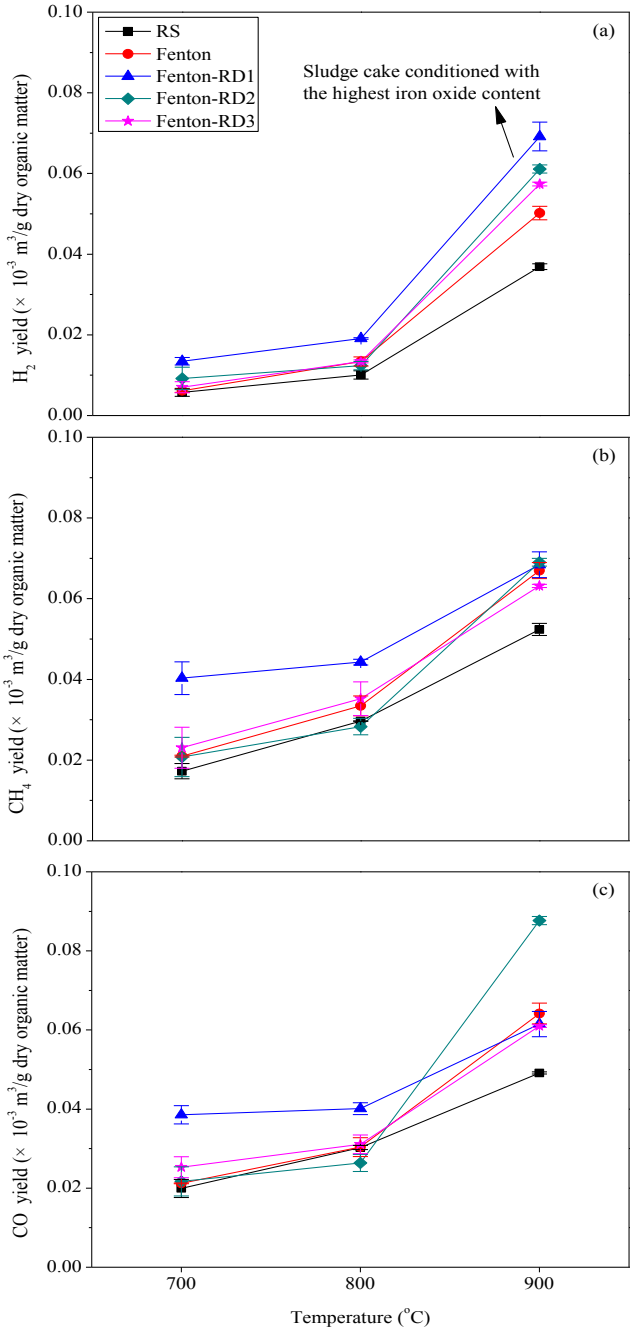

Fig. 6 – Gas yield: (a) H_2, (b) CH_4 and (c) CO in the pyrolysis of the RS and the other four sludge cakes conditioned with Fenton alone, Fenton-RD1, Fenton-RD2, and Fenton-RD3 at various temperatures.

Please cite this article in press as: Song J, et al., Red mud enhanced hydrogen production from pyrolysis of deep-dewatered sludge cakes conditioned with Fenton's reagent and red mud, International Journal of Hydrogen Energy (2016), http://dx.doi.org/10.1016/j.ijhydene.2016.06.217

water. H_2 yields are in the following order: Fenton-RD1 > Fenton-RD2 > Fenton-RD3 > Fenton > RS, as described in Fig. 6(a), thus it can be concluded that the existence of red mud in three Fenton-RD samples enhanced the hydrogen production. Regrettably, there have been few literatures explaining the mechanism that red mud could enhance H_2 production during sewage sludge pyrolysis. However, some researchers found that iron oxide had a better catalytic ability in coal gasification through the promotion of tar re-formation and char conversion, which could absolutely enhance H_2 production [26–28]. Therefore, it can be deduced that the iron oxide in red mud could enhance the hydrogen production during the sludge pyrolysis, and the higher the iron oxide content in red mud was, the more enhanced efficiency of the hydrogen production was. Furthermore, it can be found that Fenton-RD1 generally produced the higher CH_4 and CO yields, as shown in Fig. 6(b) and (c). So it implies that red mud accelerated the crack of C–C and C–H bonds between intermediate products among the complicated interactions during the pyrolysis process, which was consistent with the faster decrease of hydrocarbons from three Fenton-RD samples, compared to the RS and the Fenton samples. Some typical reactions are presented in Equations (1)–(4) below [29]. It can also be attributed to the catalytic actions of iron oxide in red mud as above explanations.

$$\text{Oil(tar)} \rightarrow \text{heavy hydrocarbons} + \text{light hydrocarbons} + CO + CO_2 + H_2 \quad (1)$$

$$\text{Heavy hydrocarbons} \rightarrow \text{light hydrocarbons} + CH_4 + H_2 \quad (2)$$

$$\text{Light hydrocarbons} \rightarrow CH_4 + H_2 \quad (3)$$

$$CH_4 \rightarrow 2H_2 + C \quad (4)$$

Tar analysis

As shown in Fig. 7, tars mainly consist of aromatic hydrocarbons, including monocyclic aromatics, polyaromatic hydrocarbon, and other benzene substituents, and a few aliphatics. The qualitative compositions of tars were essentially the same among five sludge samples at different temperatures. To further analyze the changes in tars, the identified main components were divided into six groups by summing up the peak areas in each group, and they were: (1) aliphatic hydrocarbons including cyclohexane, (2) monocyclic aromatics such as indene, benzene and their respective alkyl derivatives, (3) polyaromatic hydrocarbons (PAHs) including naphthalene, phenanthrene, pyrene, fluoranthene, triphenylene, anthracene, benzanthrene, indeno [1,2,3-cd] pyrene and their respective derivatives, (4) oxy-compounds such as fluorene-9-methanol, (5) substituted aromatics such as quinoline, indole, pyridines, isoquinoline and their respective derivatives, and (6) aromatic nitriles including aniline, benzonitrile and acridine.

As shown in Table 4, a substantial amount of substituted aromatics, aromatic nitriles and oxy-compounds were detected in the tars, indicating that proteins in the raw sludge had completely participated in the pyrolysis process. The content

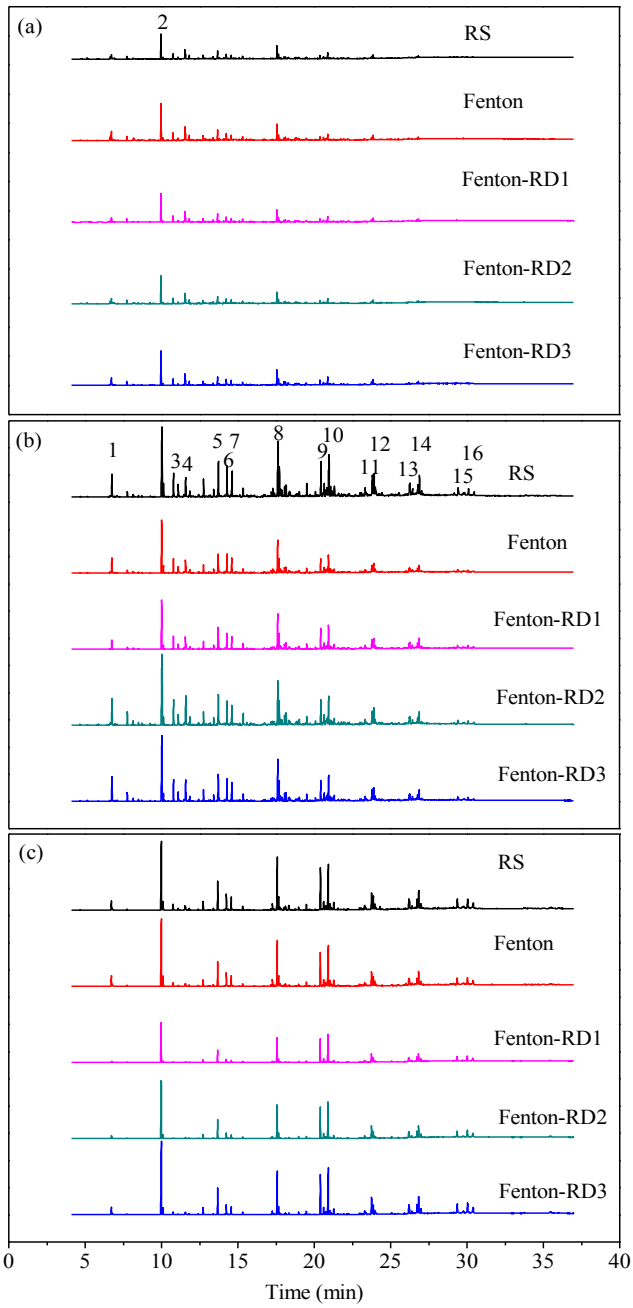

Fig. 7 – TIC of tars obtained from the pyrolysis of the RS and the other four sludge cakes conditioned with Fenton alone, Fenton-RD1, Fenton-RD2, and Fenton-RD3 at different temperatures: (a) 700 °C, (b) 800 °C and (c) 900 °C. (1-Benzonitrile, 2-Naphthalene, 3-Quinoline, 4-Indole, 5-Biphenylene, 6-Naphthalenecarbonitrile, 7-Naphthalenecarbonitrile, 8-Phenanthrene, 9-Fluoranthene, 10-Pyrene, 11-3-Bromo-7-methylbenzo(b) thiophene, 12-Triphenylene, 13-Benzo[e]pyrene, 14-Benzo [a]pyrene, 15-Indeno [1,2,3-cd]pyrene, 16-Benzo[ghi] perylene).

Please cite this article in press as: Song J, et al., Red mud enhanced hydrogen production from pyrolysis of deep-dewatered sludge cakes conditioned with Fenton's reagent and red mud, International Journal of Hydrogen Energy (2016), http://dx.doi.org/10.1016/j.ijhydene.2016.06.217

Table 4 – The relative content of six component groups of tars at three different temperatures (wt%).

Specimens	Temperature	Aliphatic hydrocarbons	Monocyclic aromatics	PAHs	Oxy-compounds	Substituted aromatics	Aromatic nitriles
RS	700 °C	0.00	4.96	53.96	0.70	30.25	10.13
	800 °C	0.00	0.46	57.24	0.00	26.37	13.91
	900 °C	0.13	0.24	73.97	2.77	15.13	7.75
Fenton	700 °C	0.00	5.07	53.94	0.91	28.20	11.87
	800 °C	0.00	1.50	54.18	1.12	22.63	20.57
	900 °C	0.00	0.18	73.92	0.27	16.34	9.29
Fenton-RD1	700 °C	0.00	3.03	56.12	0.46	29.69	10.70
	800 °C	0.17	2.20	63.56	1.79	20.42	11.86
	900 °C	0.00	0.00	88.54	0.00	7.07	4.39
Fenton-RD2	700 °C	0.85	4.74	52.84	0.00	29.55	12.02
	800 °C	0.17	2.88	54.38	1.06	26.34	15.17
	900 °C	0.00	0.00	86.28	0.00	7.38	6.35
Fenton-RD3	700 °C	0.00	2.61	54.04	0.00	14.18	29.18
	800 °C	0.00	2.18	55.69	1.09	23.92	17.13
	900 °C	0.00	0.13	82.50	0.29	11.46	5.62

of aliphatic hydrocarbons is negligible, because of its instability at high temperatures. Obviously, PAHs, considered as the feature products of tar re-formation, are the dominant components in the tars. With increasing temperature, the content of PAHs for all sludge samples increased dramatically, as shown in Fig. S1. Among different sludge samples, the relative contents of PAHs were almost the same under 700 °C. In contrast, under 800 °C, the relative content of PAHs of Fenton-RD1 increased the mostly among all five sludge samples. The relative contents of PAHs of Fenton-RD1, Fenton-RD2 and Fenton-RD3 samples were obviously higher than those of the RS and the Fenton samples at 900 °C. It indicated that red mud especially RD1 with the highest iron oxide content, promoted the formation of PAHs at higher temperatures. As formation of PAHs with increasing temperature, the Diels–Alder reaction mechanism followed by dehydrogenation as illustrated in Fig. S2, was favored by many researchers [9]. First, the heavy components of tar were transformed into alkenes and dienes, which were considered as the precursor of aromatic compounds formation via depolymerization or dehydrogenation. Subsequently, the generated alkenes and dienes were transformed into mononuclear aromatics via cyclization reactions at higher temperatures. Finally, conjugated diene and mononuclear aromatics were transformed into macromolecular polycyclic aromatic hydrocarbons via aromatization reactions. So, it could be found that red mud had accelerated the above three reactions with increasing temperature, which resulted in higher content of PAHs in tars for three Fenton-RD samples than the RS and the Fenton samples as illustrated in Fig. S1. The higher Fe_2O_3 content in red mud was, the higher content of PAHs in tar was, which was in accordance with the cracking of C–C bonds and C–H bonds that led to more H_2 yield.

Red mud samples used in this study were rich in iron-aluminum oxides, mainly in the forms of hematite (α-Fe_2O_3), and bayerite ($Al(OH)_3$) (Fig. 1). RD1, especially, contains 40.85 wt% of iron oxide. Remarkable advances were achieved in the development of iron-based catalysts that had proven a wealth of ability in tar re-formation [18,30–32]. As for the function of red mud on the PAHs formation during the sludge pyrolysis, the increase in relative content of PAHs in tar from three Fenton-RD samples should have an intimate connection of catalytic effect of iron oxides in red mud, which could accelerate reactions of dehydrogenation, cyclization to produce more precursors for PAHs formation. Furthermore, the distribution of electron cloud of π in substituted aromatics was more unstable than polyaromatic hydrocarbons, so that the substitution of a nitrogen atom into a benzene molecule created a dipole in the molecule, reducing its polarizability and the spatial extent of the electron density [33]. Some substituted aromatics would be transformed into aromatics with increasing temperature, which is in accordance with an increase in the relative content of PAHs. Fig. S3 presents some possible transformations between substituted aromatics and aromatics. The iron oxide in red mud could activate π-bond to promote the transformation process, and thus enhance H_2 production. As RD1 had a higher content of iron oxide (40.85 wt%) than RD2 (33.88 wt%) and RD3 (9.48 wt%), it performed the best in accelerating the PAHs formation and activation of electron cloud of π-bond in the substituted aromatics, thus enhancing more H_2 production.

Solid char analysis

Fig. 8 displays the FTIR spectra of solid chars from five sludge samples pyrolyzed at 700, 800 and 900 °C. As shown in Fig. 8, the absorption peaks of O–H and N–H stretching vibrations of five sludge samples between 3699 and 3296 cm^{-1} almost disappeared when temperature reached 700 °C, indicating that water and amines in the sludge samples were readily decomposed. The stretching vibration of C–H between 2925 and 2853 cm^{-1} also disappeared when temperature reached 700 °C, because the decomposition of aliphatic chain resulted in the release of some hydrocarbon gases, such as CH_4 and C_2H_4. In addition, a significant reduction of C=O absorbance at 1637 cm^{-1} with increasing temperature revealed the cracking of acids and aldehydes in the sludge samples, giving rise to the release of CO and CO_2. However, unlike other organic groups, the stretching vibrations of C–O and C–$H_{ar.}$ with absorbance at 1035 cm^{-1} and from 800 to 400 cm^{-1}, respectively, had no evident changes at 700 °C, which might be attributed to the formation of aromatic hydrocarbons [23]. Afterwards, as the increase of temperature, the IR absorbance of C–O and C–$H_{ar.}$ decreased dramatically, which might be

Please cite this article in press as: Song J, et al., Red mud enhanced hydrogen production from pyrolysis of deep-dewatered sludge cakes conditioned with Fenton's reagent and red mud, International Journal of Hydrogen Energy (2016), http://dx.doi.org/10.1016/j.ijhydene.2016.06.217

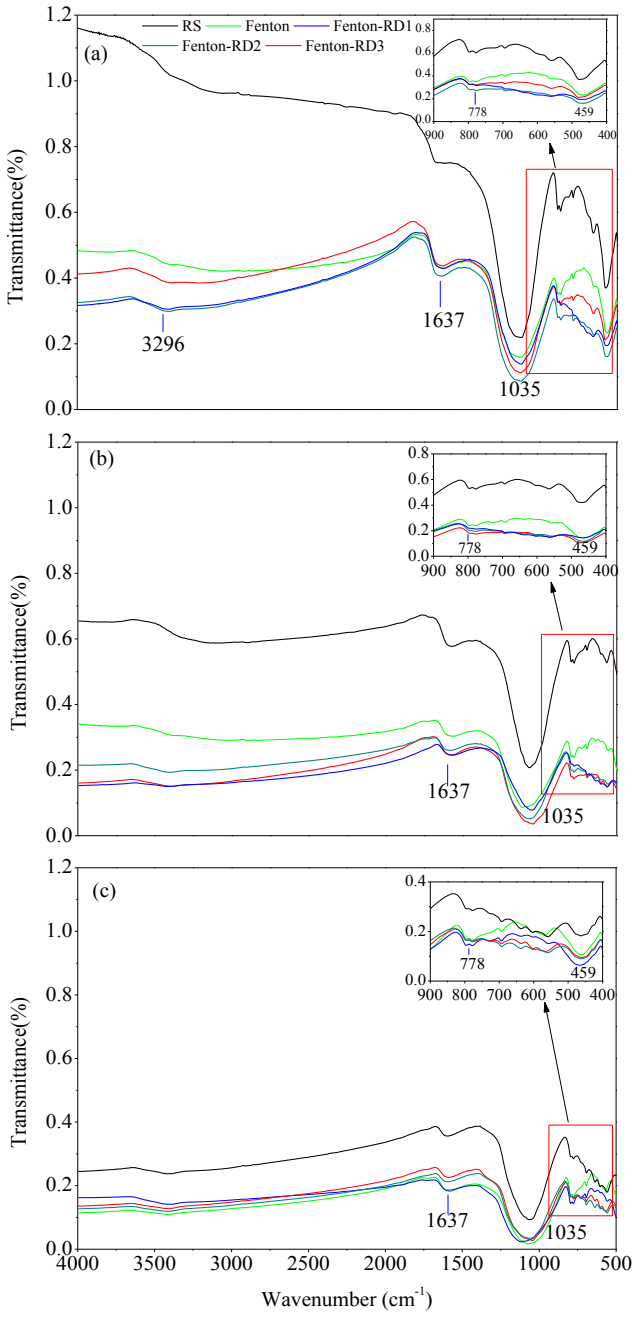

Fig. 8 – FTIR spectra of solid char of the RS and the other four sludge cakes pyrolyzed at different temperatures: (a) 700 °C, (b) 800 °C, and (c) 900 °C.

due to the cracking and reformation of aromatics leading to a release of a large amount of H_2 when the temperature increased from 700 to 900 °C. Furthermore, at 700 and 900 °C the IR absorbance of C–$H_{ar.}$ in the sludge cakes conditioned with three Fenton-RD samples was weaker than both RS and alone Fenton samples, indicating that red mud intensified the cracking and re-formation of aromatics in char. This result was consistent with relative higher content of PAHs and H_2 yield in pyrolysis tars from red mud conditioned sludge cakes in Sections "Gas production" and "Tar analysis".

Conclusions

Pyrolytic performances of deep-dewatered sludge cakes, previously conditioned with Fenton's reagent and red mud, were investigated in this study. The results showed that red mud promoted the decomposition of organics in char and accelerated the secondary cracking of tar during pyrolysis process via cyclization and aromatization reactions, leading to more hydrogen production. Moreover, the enhanced efficiency of red mud in promoting hydrogen yield had an intimate relationship with its iron oxide content. Red mud with the highest iron oxide content provided the strongest enhanced efficiency and resulted in the highest H_2 yield.

Acknowledgments

The research was supported by the Research Project of Chinese Ministry of Education (No 113046A), the National Natural Science Foundation of China (51508214), Project of Innovative and Interdisciplinary Team of HUST (2015ZDTD027) and the Foundation of State Key Laboratory of Coal Combustion (FSKLCCA1604). The authors would like to thank Analytical and Testing Center of Huazhong University of Science and Technology for providing detecting instruments.

Appendix A. Supplementary data

Supplementary data related to this article can be found at http://dx.doi.org/10.1016/j.ijhydene.2016.06.217.

REFERENCES

[1] Feng L, Luo J, Chen Y. Dilemma of sewage sludge treatment and disposal in China. Environ Sci Technol 2015;49:4781–2.
[2] Neyens E, Baeyens J, Dewil R, De heyder B. Advanced sludge treatment affects extracellular polymeric substances to improve activated sludge dewatering. J Hazard Mater 2004;106:83–92.
[3] Citeau M, Larue O, Vorobiev E. Influence of salt, pH and polyelectrolyte on the pressure electro-dewatering of sewage sludge. Water Res 2011;45:2167–80.
[4] GB/T23485. Disposal of sludge from municipal wastewater treatment plant-Quality of sludge for co-landfilling. 2009. General Administration of Quality Supervision, Inspection and Quarantine of the People's Republic of China.
[5] Gai C, Guo Y, Liu T, Peng N, Liu Z. Hydrogen-rich gas production by steam gasification of hydrochar derived from sewage sludge. Int J Hydrogen Energy 2016;41:3363–72.
[6] Zhang H, Yang J, Yu W, Luo S, Peng L, Shen X, et al. Mechanism of red mud combined with Fenton's reagent in sewage sludge conditioning. Water Res 2014;59:239–47.
[7] Smoliński A, Howaniec N. Co-gasification of coal/sewage sludge blends to hydrogen-rich gas with the application of simulated high temperature reactor excess heat. Int J Hydrogen Energy 2016;41:8154–8.
[8] Shao J, Yan R, Chen H, Wang B, Lee DH, Liang DT. Pyrolysis characteristics and kinetics of sewage sludge by

thermogravimetry Fourier transform infrared analysis†. Energy Fuels 2007;22:38–45.
[9] Zhang B, Xiong S, Xiao B, Yu D, Jia X. Mechanism of wet sewage sludge pyrolysis in a tubular furnace. Int J Hydrogen Energy 2011;36:355–63.
[10] He C, Wang K, Giannis A, Yang Y, Wang J-Y. Products evolution during hydrothermal conversion of dewatered sewage sludge in sub- and near-critical water: effects of reaction conditions and calcium oxide additive. Int J Hydrogen Energy 2015;40:5776–87.
[11] Choi Y-K, Cho M-H, Kim J-S. Air gasification of dried sewage sludge in a two-stage gasifier. Part 4: application of additives including Ni-impregnated activated carbon for the production of a tar-free and H_2-rich producer gas with a low NH_3 content. Int J Hydrogen Energy 2016;41:1460–7.
[12] Liu H, Zhang Q, Hu H, Li A, Yao H. Influence of residual moisture on deep dewatered sludge pyrolysis. Int J Hydrogen Energy 2014;39:1253–61.
[13] Jollet V, Gissane C, Schlaf M. Optimization of the neutralization of red mud by pyrolysis bio-oil using a design of experiments approach. Energy Environ Sci 2014;3:1125–33.
[14] Liu W, Chen X, Li W, Yu Y, Yan K. Environmental assessment, management and utilization of red mud in China. J Clean Prod 2014;84:606–10.
[15] Liu X, Zhang N. Utilization of red mud in cement production: a review. Waste Manag Res 2011;29:1053–63.
[16] Halász J, Hodos M, Hannus I, Tasi G, Kiricsi I. Catalytic detoxification of C_2-chlorohydrocarbons over iron-containing oxide and zeolite catalysts. Coll Surf A Physicochem Eng Asp 2005;265:171–7.
[17] Eamsiri A, Jackson WR, Pratt KC, Christov V, Marshall M. Activated red mud as a catalyst for the hydrogenation of coals and of aromatic compounds. Fuel 1992;71:449–53.
[18] Yathavan BK, Agblevor F. Catalytic pyrolysis of Pinyon–Juniper using red mud and HZSM-5. Energy Fuels 2013;27:6858–65.
[19] López A, De Marco I, Caballero B, Laresgoiti M, Adrados A, Aranzabal A. Catalytic pyrolysis of plastic wastes with two different types of catalysts: ZSM-5 zeolite and red mud. Appl Catal B Environ 2011;104:211–9.
[20] Balakrishnan M, Batra V, Hargreaves J, Monaghan A, Pulford I, Rico J, et al. Hydrogen production from methane in the presence of red mud–making mud magnetic. Green Chem 2009;11:42–7.
[21] Álvarez J, Ordóñez S, Rosal R, Sastre H, Díez FV. A new method for enhancing the performance of red mud as a hydrogenation catalyst. Appl Catal A General 1999;180:399–409.
[22] Domínguez A, Menéndez JA, Inguanzo M, Pís JJ. Production of bio-fuels by high temperature pyrolysis of sewage sludge using conventional and microwave heating. Bioresour Technol 2006;97:1185–93.
[23] Li J, Yan R, Xiao B, Wang X, Yang H. Influence of temperature on the formation of oil from pyrolyzing palm oil wastes in a fixed bed reactor. Energy Fuels 2007;21:2398–407.
[24] Azhar Uddin M, Tsuda H, Wu S, Sasaoka E. Catalytic decomposition of biomass tars with iron oxide catalysts. Fuel 2008;87:451–9.
[25] Wu Q, Zhang C, Zhang B, Li X, Ying Z, Liu T, et al. Highly selective Pt/ordered mesoporous TiO_2-SiO_2 catalysts for hydrogenation of cinnamaldehyde: the promoting role of Ti^{2+}. J Colloid Interface Sci 2016;463:75–82.
[26] Ohtsuka Y, Asami K. Highly active catalysts from inexpensive raw materials for coal gasification. Catal Today 1997;39:111–25.
[27] Ohtsuka Y, Asami K. Steam gasification of low-rank coals with a chlorine-free iron catalyst from ferric chloride. Ind Eng Chem Res 1991;30:1921–6.
[28] Yu J, Tian F-J, Chow MC, McKenzie LJ, Li C-Z. Effect of iron on the gasification of Victorian brown coal with steam: enhancement of hydrogen production. Fuel 2006;85:127–33.
[29] Leung DYC, Yin XL, Zhao ZL, Xu BY, Chen Y. Pyrolysis of tire powder: influence of operation variables on the composition and yields of gaseous product. Fuel Process Technol 2002;79:141–55.
[30] Sushil S, Batra VS. Catalytic applications of red mud, an aluminium industry waste: a review. Appl Catal B Environ 2008;81:64–77.
[31] Dulger Irdem S, Parparita E, Vasile C, Uddin MA, Yanik J. Steam reforming of tar derived from walnut shell and almond shell gasification on red mud and iron–ceria catalysts. Energy Fuels 2014;28:3808–13.
[32] Khelfa A, Sharypov V, Finqueneisel G, Weber JV. Catalytic pyrolysis and gasification of Miscanthus Giganteus: haematite (Fe_2O_3) a versatile catalyst. J Anal Appl Pyrolysis 2009;84:84–8.
[33] Hohenstein EG, Sherrill CD. Effects of heteroatoms on aromatic π-π interactions: benzene-pyridine and pyridine dimer. J Phys Chem A 2009;113:878–86.

Please cite this article in press as: Song J, et al., Red mud enhanced hydrogen production from pyrolysis of deep-dewatered sludge cakes conditioned with Fenton's reagent and red mud, International Journal of Hydrogen Energy (2016), http://dx.doi.org/10.1016/j.ijhydene.2016.06.217